Combustion and Flame xxx (2015) xxx–xxx

Contents lists available at ScienceDirect

Combustion and Flame

journal homepage: www.elsevier.com/locate/combustflame

Effects of finite-rate droplet evaporation on the ignition and propagation of premixed spherical spray flame

Wang Han [a], Zheng Chen [a,b,*]

[a] State Key Laboratory for Turbulence and Complex Systems, Department of Mechanics and Engineering Science, College of Engineering, Peking University, Beijing 100871, China
[b] Department of Aeronautics and Astronautics, College of Engineering, Peking University, Beijing 100871, China

ARTICLE INFO

Article history:
Received 5 November 2014
Received in revised form 19 January 2015
Accepted 20 January 2015
Available online xxxx

Keywords:
Spherical spray flame
Finite-rate evaporation
Ignition
Flame propagation speed
Markstein length

ABSTRACT

Droplet evaporation might have great impact on fundamental spray combustion processes such as ignition, flame propagation, and extinction. In this study, we adopt and analyze a simplified model for spherical spray flame initiation and propagation in an overall fuel-rich or fuel-lean pre-mixture containing fuel droplet with finite-rate evaporation, fuel vapor, and air. We consider the limit of small droplets such that the medium can be considered as a continuum and adopt the sectional approach to model poly-disperse spray. Moreover, the thermal-diffusive model with constant density is employed and the spherical flame is assumed to propagate in a quasi-steady state. Under these assumptions, analytical correlations describing the change of flame propagation speed with flame radius are derived for the premixed spherical spray flame. The initial droplet load, vaporization Damköhler number, Lewis number, and ignition power are included in these correlations. Based on these correlations, spherical spray flame initiation and propagation are investigated with the emphasis on assessing the impact of droplet evaporation at different Lewis numbers. It is found that the spray flame propagation speed, Markstein length, and minimum ignition power are affected in different ways by the initial droplet load and vaporization Damköhler number and that the influence depends on Lewis number. Moreover, the influence of droplet evaporation on the fuel-lean case is greatly different from that on the fuel-rich case. This is mainly due to the facts that the fuel-rich spherical spray flame is affected by droplet evaporation only through latent heat of vaporization absorbed in the pre-flame and post-flame zones; while the fuel-lean spherical spray flame is affected by droplet evaporation through (1) latent heat of vaporization absorbed in the pre-flame and post-flame zones and (2) change in local effective equivalence ratio. For hydrocarbon fuels with large Lewis number, the lean spray flame is much more difficult to be ignited compare to the equivalent purely gaseous flame.

1. Introduction

Relight during flight is one of the most important problems in jet-engine and it becomes even more critical in the oxygen/fuel deficiency and the presence of liquid fuel or water droplets. Droplet evaporation might have great impact on ignition and flame propagation processes. The realistic systems contain poly-disperse sprays and turbulent flows, for which investigation on spray flame initiation and propagation processes can be undertaken only by numerical simulation. Unfortunately, numerical simulation is usually limited to specific fuel and conditions, and hence the conclusions are lack of generality. To get a general understanding of spray combustion, here we conduct theoretical analysis on a deliberately simplified model for spherical spray flame initiation and propagation. Since the spark ignition process can be approximately modeled as spherical flame initiation and propagation, the spherical spray flame initiation and propagation can be used to assess the effects of droplet evaporation on fundamental spray combustion processes.

In the literature there are many studies on spray flame propagation. Continillo and Sirignano [1,2] first numerically examined the spherical flame propagation in a fuel spray mixture and found that multiple flames occur in spray combustion. Chiu and Lin [3] investigated the transient poly-disperse fuel droplet cluster combustion. Lin et al. [4,5] analyzed steady-state propagation of one-dimensional mono-disperse spray flames in off-stoichiometric mixtures. Kalma and coworkers [6,7] reported the time evolution

* Corresponding author at: State Key Laboratory for Turbulence and Complex Systems, Department of Mechanics and Engineering Science, College of Engineering, Peking University, Beijing 100871, China.
E-mail address: cz@pku.edu.cn (Z. Chen).

http://dx.doi.org/10.1016/j.combustflame.2015.01.011
0010-2180/

Nomenclature

A	pre-factor of reaction
C	sectional vaporization coefficient
C_P	specific heat at constant pressure
D	Fick diffusion coefficient
Da	vaporization Damköhler number
E	evaporation-related integral (see Eq. (29))
F	gaseous fuel
f_i	amount of evaporation (i = 1, 2, 3)
H	Heaviside function
I_1, I_2	integral function (see Eq. (28))
K	flame stretch rate
L	Markstein length
l_0^{ad}	flame thickness of an adiabatic planar flame
Le	Lewis number
O	oxygen
Q	ignition power
q_c	reaction heat-release per unit mass of the deficient reactant
q_v	latent heat of vaporization
R^0	universal gas constant
R_f	flame radius
R_v	front of onset vaporization
S_{ad}^0	laminar flame speed of an adiabatic planar flame
T	temperature
T_{ad}^0	flame temperature of an adiabatic planar flame
T_v	reference temperature (close to the boiling temperature)
t, r	temporal and spatial coordinates
U	flame propagation speed
Z	Zel'dovich number

Greek letters

α	parameter used to distinguish the fuel rich (α=0) and fuel-lean (α=1) cases
δ	initial droplet load
η	moving coordinate attached to the propagating flame front
η_v	location of the front of onset vaporization in the moving coordinate
λ	heat conductivity of the mixture
ν	molar stoichiometric coefficient
ρ	density of the mixture
σ	thermal expansion ratio
ω_c	chemical reaction rate
ω_v	finite evaporation rate
ϖ	droplet-burning-related sink term (see Eq, (9))
Δ_M	thicknesses for mass diffusion
Δ_T	thicknesses for temperature diffusion

Superscripts

$\sim$	dimensional quantity
0	at zero stretch rate

Subscripts

c	critical quantity
d	corresponding to the liquid fuel (droplet)
F	corresponding to the gaseous fuel
f	at the flame front
O	corresponding to the oxygen
u	quantity in the fresh mixture
v	at the front of onset vaporization

of spherical propagating poly-disperse spray flames using the sectional approach [8]. Bradley et al. [9] experimentally assessed the mass burning velocities, entrainment velocities and flame instabilities of the aerosols using the propagating spherical flame. Greenberg and coworkers [8,10–17] systematically analyzed the propagation of planar and spherical spray flames using slowly varying flame (SVF) approach. Specifically, stoichiometry and poly-disperse effects were examined and a heterogeneous-dominated burning velocity formula were reported in [8,10]; the combined effects of heat loss induced by droplet evaporation and radiation on the extinction of fuel-rich spherical spray flame were addressed in [12]; the effects of finite-rate evaporation and droplet drag on fuel-rich flame propagation were assessed in [14]; the influence of stretch rate on poly-disperse spherical spray flames was investigated for the first time in [17]. In these studies, droplet evaporation was found to strongly affect flame propagation. However, highly stretched spray flames with small flame radius were not considered in these studies and thereby the ignition kernel development after spark was not investigated. To the authors' knowledge, in the literature there are few theoretical studies on the ignition of spray flames especially for the fuel-lean case. Therefore, spray flame initiation for both fuel-rich and fuel-lean cases will be explored in this study.

Lefebvre and coworkers [18–20] conducted a series of experimental and numerical studies on spark ignition of heterogeneous mixtures. When a kerosene-air mixture was ignited by spark, the minimum ignition power was found to be affected by fuel volatility and initial droplet load. Ballal and Lefebvre [19] showed that under certain conditions the spray flame initiation process is vaporization-dominated rather than kinetically-dominated. Aggarwal and coworkers [21–23] numerically studied the effects of the initial droplet size, equivalence ratio, and fuel volatility on spray flames. A comprehensive review of previous numerical studies on spray ignition phenomena was conducted by Aggarwal [24]. More recently, Neophytou and Mastorakos [25] have numerically studied one-dimensional planar flame propagation in sprays of *n*-heptane and *n*-decane with detailed chemistry and transport. It is found that the maximum speed is achieved with small droplet diameter and long residence time under fuel-lean conditions. Neophytou [26] gave a literature review on ignition and flame propagation in sprays and conducted direct numerical simulations of combustion in laminar and turbulent sprays. Though many numerical studies were conducted in the literature, the effects of initial droplet load, finite-rate evaporation, and Lewis number on spray flame initiation are still not well understood.

The present work aims to develop a simplified theoretical description of spherical spray flame initiation and propagation and to assess the effects of droplet evaporation for both fuel-rich and fuel-lean cases. The focus is on examining how the spherical flame propagation speed, Markstein length, and minimum ignition power are affected by the initial droplet load and vaporization Damköhler number at different Lewis numbers. It is noted that many assumptions are made in theoretical analysis and thereby qualitative instead of quantitative information can be provided. Nevertheless, the theoretical analysis on ignition and propagation of spray flames will be helpful to understand the underlying mechanisms and to give physical insight into the relight problem.

The rest of the paper is organized as follows. The mathematical model and analytical solution are introduced in the next section. In Section 3, the propagating spherical spray flame without and with ignition power deposition at the center are analyzed for both

fuel-rich and fuel-lean cases. Finally, the conclusions are summarized in Section 4.

2. Theoretical analysis

2.1. Mathematical model

We consider a simplified model for one-dimensional spherical spray flame initiation and propagation in an unconfined domain containing fuel droplet, fuel vapor, and air. A self-sustained outwardly propagating spherical flame can be established through successful ignition at the center. As discussed in [8,10,25,27] and shown in Figs. 1 and 2, the flame structure consists of a pre-vaporization zone (in which droplet evaporation is assumed to be negligible), a pre-flame zone (in which finite-rate vaporization occurs), a thin reaction zone (which is considered as a reaction sheet at large-activation energy) and a post-flame zone. The front of onset of vaporization is located at the radius of $\widetilde{R}_v$ and the flame front is at $\widetilde{R}_f$. The equivalence ratio can be defined in different ways since both fuel vapor and droplets exist. In this study, fuel-rich and fuel-lean refer to the equivalence ratio based on total fuel concentration composed of both fuel vapor and droplet; while the effective equivalence ratio is based on only the fuel vapor concentration. For the fuel-rich case with local effective equivalence ratio at the flame front above unity, oxygen is completely consumed. In this case, the droplets that traverse the flame front will enter an oxygen-depleted zone and they will continue to vaporize in the post-flame zone without droplet burning (see Fig. 1). For the fuel-lean case, the local effective equivalence ratio at the flame front is always below unity and therefore the droplets, after being ignited while traversing through the main flame zone, will first vaporize and then instantly burn individually or in cluster in the so-called heterogeneous combustion mode [8,28] in the post-flame zone. Accordingly, for the fuel-rich case, gaseous fuel supply due to droplet evaporation occurs in the both pre-flame and post-flame zones while for the fuel-lean case, gaseous fuel supply due to droplet evaporation only occurs in the pre-flame zone. It is noted that for the fuel-rich case, the effective equivalence ratio might be less than unity due to insufficient fuel vapor provided by the slowly droplet evaporation. This case and near-stoichiometry cases are not considered here.

The main assumptions for the present model are described below. A global, irreversible, one-step reaction described by the Arrhenius law is employed:

$$\nu_F \mathrm{F} + \nu_O \mathrm{O} \rightarrow \text{products} \qquad (1)$$

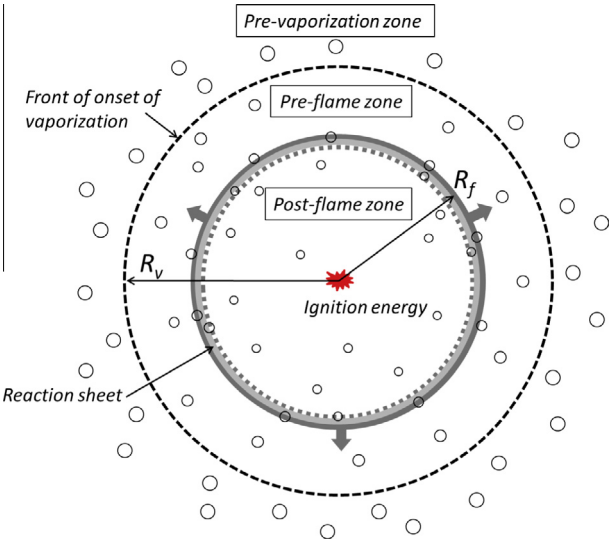

Fig. 1. Configuration for premixed spherical spray flame with finite-rate droplet evaporation. Adapted from [9,14].

where F and O represent the fuel and oxygen, respectively, and ν_i (i = F, O) the corresponding stoichiometric coefficients. Similar to previous theoretical studies (e.g. [12,14,29]), we consider the limit of small droplets such that the medium can be considered as a continuum composed of three species: air, gaseous fuel, and liquid fuel. The droplets are viewed from a far-filed vantage point (i.e., in the dilute spray region) and are considered to be dilute (i.e., its volume fraction is relatively small). Therefore, the viscosity of the liquid and interactions among the droplets are negligible and dynamic adjustment to equilibrium with their surroundings is instantaneous and their average velocity is close to that of their host environment. This simplification was validated and popularly used in previous studies [6,10,14,19,20,28,30–34]. Meanwhile, it is expected immediate adjustment of the spray's droplets to the temperature of their environment since the thermal conductivity of the liquid phase is much greater than that of the host gas phase [13–15]. Therefore, the droplets are assumed to have the same velocity and temperature as the host gas. Nevertheless, this is a limitation of theoretical analysis compared to detailed simulation which can include the heat transfer between droplet and gas phase. It is noted that the spray flame configuration considered in this paper is different from the internal group combustion mode discussed by Chiu and coworkers [3]: the former mainly describes

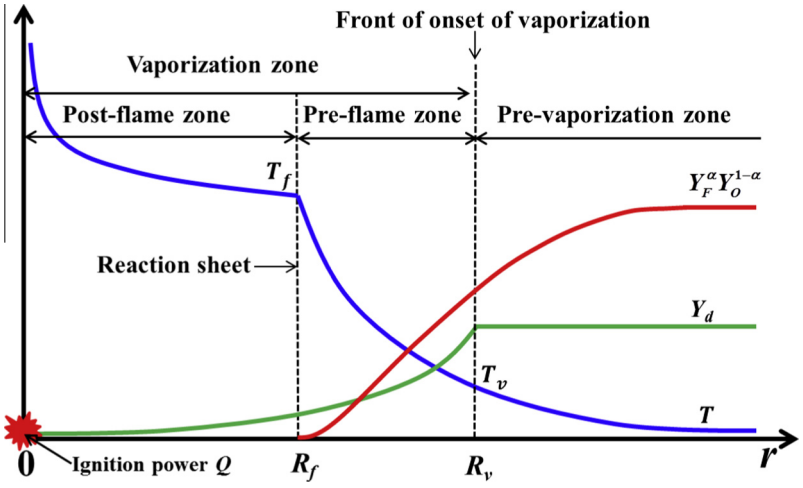

Fig. 2. Schematic of different zones and temperature and mass fraction distributions in a premixed spherical spray flame for fuel-rich (α = 0) and fuel-lean (α = 1) cases.

Please cite this article in press as: W. Han, Z. Chen, Combust. Flame (2015), http://dx.doi.org/10.1016/j.combustflame.2015.01.011

dilute spray combustion with a dominant premixed propagation flame while the latter is for dense spray combustion with a dominant diffusion flame.

Furthermore, the transport properties will be supposed to be determined primarily by the properties of the gaseous species [14,28]. This follows from the implicit assumption that the liquid fuel volume fraction is sufficiently small. For the sake of simplicity, this paper deals with the well-known diffusive-thermal model [35], according to which the density and thermal and transport properties are all assumed to be constant. In the diffusive-thermal model, the gas motion induced by thermal-expansion is neglected. Moreover, the gas motion due to droplet vaporization is also neglected. We use the parameter α to distinguish the fuel-rich ($\alpha = 0$) and fuel-lean ($\alpha = 1$) cases. Under these assumptions, the governing equations for temperature and mass fractions of different species are

$$\text{Temperature}: \tilde{\rho}\widetilde{C}_P\frac{\partial\widetilde{T}}{\partial\tilde{t}} = \frac{1}{\tilde{r}^2}\frac{\partial}{\partial\tilde{r}}\left(\tilde{r}^2\tilde{\lambda}\frac{\partial\widetilde{T}}{\partial\tilde{r}}\right) + \tilde{q}_c\tilde{\omega}_c - \tilde{q}_v\tilde{\omega}_v + \alpha\cdot\tilde{q}_c\tilde{\varpi} \tag{2}$$

$$\text{Oxygen}: \tilde{\rho}\frac{\partial\widetilde{Y}_O}{\partial\tilde{t}} = \frac{1}{\tilde{r}^2}\frac{\partial}{\partial\tilde{r}}\left(\tilde{r}^2\tilde{\rho}\widetilde{D}_O\frac{\partial\widetilde{Y}_O}{\partial\tilde{r}}\right) - \tilde{\omega}_c \tag{3}$$

$$\text{Gaseous fuel}: \tilde{\rho}\frac{\partial\widetilde{Y}_F}{\partial\tilde{t}} = \frac{1}{\tilde{r}^2}\frac{\partial}{\partial\tilde{r}}\left(\tilde{r}^2\tilde{\rho}\widetilde{D}_F\frac{\partial\widetilde{Y}_F}{\partial\tilde{r}}\right) - \tilde{\omega}_c + \tilde{\omega}_v - \alpha\cdot\tilde{\varpi} \tag{4}$$

$$\text{Liquid fuel}: \tilde{\rho}\frac{\partial\widetilde{Y}_d}{\partial\tilde{t}} = -\tilde{\omega}_v \tag{5}$$

where $\tilde{t}$ and $\tilde{r}$ are temporal and spatial coordinates, respectively, $\widetilde{Y}_F$ the mass fraction of gaseous fuel, $\widetilde{Y}_O$ the mass fraction of oxygen, and $\widetilde{Y}_d$ the mass fraction of liquid fuel (droplet). The density, $\tilde{\rho}$, heat capacity, $\widetilde{C}_P$, heat conductivity of the mixture, $\tilde{\lambda}$, molecular diffusivity of oxygen, $\widetilde{D}_O$, and molecular diffusivity of gaseous fuel, $\widetilde{D}_F$, are all assumed to be constant in the diffusive-thermal model. The parameters, $\tilde{q}_c$ and $\tilde{q}_v$, denote the reaction heat-release per unit mass of the deficient reactant (oxygen for fuel-rich case and fuel for fuel-lean case) and the latent heat of vaporization per unit mass of droplet fuel, respectively. Adiabatic flame propagation is considered and thereby radiative loss is not included in the present model.

For simplicity and without loss of generality, the chemical reaction is assumed to be first order and only depend on the deficient reactant [34,36–40]. Therefore, for fuel-rich case only equations (2), (3) and (5) are considered while for fuel-lean case only equations (2), (4) and (5) need to be solved. The chemical reaction rate can be written as

$$\tilde{\omega}_c = \tilde{\rho}\widetilde{A}\widetilde{Y}_F^{\alpha}\widetilde{Y}_O^{1-\alpha}\exp(-\widetilde{E}/\widetilde{R}^0\widetilde{T}) \tag{6}$$

in which $\widetilde{A}$ is the pre-factor, $\widetilde{E}$ the activation energy, and $\widetilde{R}^0$ the universal gas constant.

The sectional approach modeling poly-disperse spray [10,31,32] is adopted here. The details of its development have been copiously recorded elsewhere [10,31,32] and the readers are referred to these references for more information. In order to simply assess the effects of primary spray parameters (vaporization rate and initial droplet load), the concept of a quasi-mono-disperse spray [14] (i.e., containing droplets of approximately the same size) is utilized here, although a multi-sectional poly-disperse spray model can be accommodated at the expense of algebraic complexity. Furthermore, the transient droplet heating and vaporization are not considered in the present theoretical analysis. Under the above assumptions, the finite evaporation rate, $\tilde{\omega}_v$, can be written as [14]

$$\tilde{\omega}_v = \tilde{\rho}\widetilde{C}\widetilde{Y}_d H(\widetilde{T} - \widetilde{T}_v) \tag{7}$$

where H is the Heaviside function. $\widetilde{T}_v$ is the reference temperature (close to the boiling temperature) beyond which the liquid fuel initially vaporizes. The sectional vaporization coefficient, $\widetilde{C}$, is [32,41]

$$\widetilde{C} = \left(\frac{3\pi^2}{4}\right)^{1/3}\Phi(\widetilde{T})\left[\frac{3}{4}(V_H^{4/3} - V_L^{4/3}) + V_L^{4/3}\right]\times(V_H^2 - V_L^2)^{-1/2} \tag{8}$$

where V_H and V_L are the volume of the largest and smallest droplets in the spray, respectively, and $\Phi(\widetilde{T})$ is a temperature-dependent coefficient of evaporation [41]. The latter may be determined based on theoretical or experimental data. The expression for $\widetilde{C}$ is based on the d^2-law for evaporation [32,41]. Reasonably accurate estimation of droplet size and vaporization time does demonstrate the validity of this expression, even under transient temperature conditions [42–45]. Moreover, Labowsky [44] showed that the d^2-law can approximately predict the vaporization history in the initial period of combustion and it can be significantly modified by the close presence of neighboring droplets. In this study, dilute droplets with relatively low droplet load is considered. Therefore, the effect of close presence of neighboring droplets on vaporization is expected not to be dominant and it is neglected in the present theoretical analysis. Annamalzai and Ryan [45] further confirmed Labowsky's findings. The sectional vaporization coefficient, $\widetilde{C}$, captures within it information about the volatility of the liquid fuel and the size of droplets in the spray [8,46]. Adopting d^2-law in the mono-sectional model of the spray leads to a constant averaged value of the vaporization coefficients. Greenberg [14] showed that this simplification does not affect the qualitative nature of the prediction.

In Eq. (4), the sink term $\tilde{\varpi}$ denotes the consumption of fuel vapor due to droplet burning in the post-flame zone, which only happens for the fuel-lean case (i.e. $\alpha = 1$) and in the burned zone (i.e. $r < R_f$). We assume the fuel vapor from droplet vaporization is totally consumed by the surrounding spherical diffusion flame during single droplet burning. This means that the fuel vaporization source term is equal to the fuel vapor sink term due to the diffusion flame. The source term and sink term cancel out and thereby the droplet-related source term in Eq. (4) is zero (i.e. $\tilde{\omega}_v - \alpha\tilde{\varpi} = 0$) in the post-flame zone. Therefore, the droplet-burning-related sink term in Eq. (4) is

$$\tilde{\varpi} = \tilde{\omega}_v H(\tilde{R}_f - \tilde{r}) \tag{9}$$

The impact of external energy deposition on spherical spray flame initiation and propagation is investigated. The ignition power is provided as a heat flux at the center [37,47,48]:

$$-\left(4\pi\tilde{r}^2\tilde{\lambda}\frac{\partial\widetilde{T}}{\partial\tilde{r}}\right)_{\tilde{r}\to 0} = \widetilde{Q} \tag{10}$$

This is a limitation of theoretical analysis since practically the ignition power deposition is a function of time and space. The employment of such a steady-state energy deposition is for the purpose to obtain analytical solution [37]. Nevertheless, as demonstrated by transient numerical simulations [37,47–49], this simplification does not prevent the model from predicting qualitatively correct results.

We introduce the following non-dimensional variables

$$u = \frac{\tilde{u}}{\tilde{u}_{ad}^0}\quad r = \frac{\tilde{r}}{\tilde{l}_{ad}^0}\quad t = \frac{\tilde{t}}{\tilde{l}_{ad}^0/\tilde{u}_{ad}^0}\quad Y_O = \frac{\widetilde{Y}_O}{\widetilde{Y}_{O,u}}\quad Y_F = \frac{\widetilde{Y}_F}{\widetilde{Y}_{F,u} + \widetilde{Y}_{d,u}}\quad Y_d = \frac{\widetilde{Y}_d}{\widetilde{Y}_{F,u} + \widetilde{Y}_{d,u}}\quad T = \frac{\widetilde{T} - \widetilde{T}_u}{\widetilde{T}_{ad}^0 - \widetilde{T}_u} \tag{11}$$

where $\widetilde{T}_u$, $\widetilde{Y}_{O,u}$, $\widetilde{Y}_{F,u}$ and $\widetilde{Y}_{d,u}$ denote the temperature and mass fractions in the fresh mixture, respectively. The total fuel mass fraction (i.e., droplets and fuel vapor) is $\widetilde{Y}_{F,u} + \widetilde{Y}_{d,u}$. The characteristic speed $\tilde{u}_{ad}^0$, characteristic length $\tilde{l}_{ad}^0 = \tilde{\lambda}/(\tilde{\rho}\widetilde{C}_P\tilde{u}_{ad}^0)$, and characteristic

temperature $\widetilde{T}^0_{ad}=\widetilde{T}_u+\tilde{q}_c(\widetilde{Y}_{F,u}+\widetilde{Y}_{d,u})^{\alpha}\widetilde{Y}^{1-\alpha}_{O,u}/\widetilde{C}_P$, are the laminar flame speed, flame thickness, and flame temperature of an adiabatic planar flame without fuel droplets.

We can study spherical flame propagation in the coordinate attached to the propagating flame front, R_f. In this moving coordinate, $\eta = r - R_f(t)$, the flame can be considered as in a quasi-steady state (the validation of this quasi-steady assumption has been demonstrated by transient numerical simulation for gaseous combustion without droplets [37]). It is noted that there exists a thick zone of vaporization, mixing, and reaction in flame propagating through a purely fuel spray-air mixture, which was numerically investigated by Continillo and Sirignano [1,2]. However, unlike the case containing purely fuel spray and air [1,2], in the present study the initial fuel contains not only dilute liquid fuel (small droplets) but also gaseous fuel. Since the fraction of liquid fuel is much less than that of the gaseous fuel (e.g. initial droplet load of $\delta = 0.2$), homogeneous combustion is predominated and the presence of droplets has relatively weak influence on the thickness of the flame zone [8,14,25–28]. Therefore, quasi-steady assumption is still suitable for the special case considered in the present study. As a result, the non-dimensional governing equations become

$$-U\frac{dT}{d\eta}=\frac{1}{(\eta+R_f)^2}\frac{d}{d\eta}\left[(\eta+R_f)^2\frac{dT}{d\eta}\right]+\omega_c-q_v\omega_v+\alpha\varpi \tag{12}$$

$$-U\frac{dY_O}{d\eta}=\frac{Le_O^{-1}}{(\eta+R_f)^2}\frac{d}{d\eta}\left[(\eta+R_f)^2\frac{dY_O}{d\eta}\right]-\omega_c \tag{13}$$

$$-U\frac{dY_F}{d\eta}=\frac{Le_F^{-1}}{(\eta+R_f)^2}\frac{d}{d\eta}\left[(\eta+R_f)^2\frac{dY_F}{d\eta}\right]-\omega_c+\omega_v-\alpha\varpi \tag{14}$$

$$-U\frac{dY_d}{d\eta}=-\omega_v \tag{15}$$

where $U = dR_f(t)/dt$ is the non-dimensional flame propagation speed. $Le_F=\tilde{\lambda}/(\tilde{\rho}\widetilde{C}_P\widetilde{D}_F)$ and $Le_O=\tilde{\lambda}/(\tilde{\rho}\widetilde{C}_P\widetilde{D}_O)$ are respectively the Lewis numbers of fuel and oxygen.

The normalized reaction rate in Eqs. (12)–(14) is

$$\omega_c=\frac{Le_O^{\alpha-1}}{2Le_F^{\alpha}}\cdot Y_F^{\alpha}\cdot Y_O^{1-\alpha}\cdot Z^2\cdot\exp\left[\frac{Z(T-1)}{\sigma+(1-\sigma)T}\right] \tag{16}$$

where Z is the Zel'dovich number, σ the thermal expansion ratio (the density ratio between burned and unburned gases).

The normalized latent heat of vaporization and evaporation rate are

$$q_v=\tilde{q}_v(\widetilde{Y}_{F,u}+\widetilde{Y}_{d,u})^{1-\alpha}\widetilde{Y}^{\alpha-1}_{O,u}/\tilde{q}_c \tag{17}$$

$$\omega_v=DaY_dH(T-T_v) \tag{18}$$

Here $Da=\widetilde{C}\tilde{\delta}^0_f/\tilde{S}^0_u$ is the vaporization Damköhler number, which is the ratio between the characteristic time of flame and that of evaporation. In the mono-sectional spray model, Da increases with the volatility of the fuel and decreases with the droplet size. Therefore, faster vaporization occurs at larger Da.

The normalized droplet-burning-related sink term in Eq. (14) is

$$\varpi=\omega_vH(-\eta) \tag{19}$$

2.2. Matching and boundary conditions

Figure 2 shows the distributions of different variables that need to be considered. According to Fig. 2, the non-dimensional boundary conditions are

$$\eta=-R_f,\quad (\eta+R_f)^2dT/d\eta=-Q,\quad dY_F/d\eta=dY_O/d\eta=0 \tag{20}$$

$$\eta\to\infty,\quad T=0,\quad Y_d=\delta,\quad Y_F=1-\delta,\quad Y_O=1 \tag{21}$$

At the vaporization front, $\eta = \eta_v$, T, Y_F, Y_O, and Y_d satisfy the following matching conditions

$$T=T_v,[\![Y_d]\!]=[\![Y_F]\!]=[\![Y_O]\!]=[\![T]\!]=[\![dY_O/d\eta]\!]=[\![dY_F/d\eta]\!]=[\![dT/d\eta]\!]=0 \tag{22}$$

where the square brackets $[\![\cdot]\!]$ denote the difference between the variables on both sides of the vaporization front or reaction sheet; $\eta_v = R_v - R_f$ denotes the location of the evaporation front where temperature reaches the boiling point of the liquid fuel; δ is the initial droplet load defined as $\delta=\widetilde{Y}_{d,u}/(\widetilde{Y}_{F,u}+\widetilde{Y}_{d,u})$.

In the limit of large activation energy, chemical reaction occurs only within a very thin zone of high temperature and at the flame sheet (i.e., $\eta = 0$) the jump relations for the non-dimensional temperature and mass fraction are given by [35,40,53]

$$T=T_f,\quad Y_F^{\alpha}Y_O^{1-\alpha}=[\![Y_d]\!]=0 \tag{23}$$

$$-\left[\!\left[\frac{dT}{d\eta}\right]\!\right]=\frac{Le_O^{\alpha-1}}{Le_F^{\alpha}}\left[\!\left[\frac{d(Y_F^{\alpha}Y_O^{1-\alpha})}{d\eta}\right]\!\right]=[\sigma+(1-\sigma)T_f]^2\exp\left[\frac{Z}{2}\frac{T_f-1}{\sigma+(1-\sigma)T_f}\right] \tag{24}$$

where T_f is the flame temperature (which depends on the concentration of the deficient reactant and other factors).

Equations (12)–(15) subject to boundary/matching conditions in Eqs. (20)–(24) can be solved analytically. The results are presented in the following subsection.

2.3. Analytical solution

For the fuel-rich case ($\alpha = 0$), oxygen is completely consumed at the flame front and only Eqs. (12), (13) and (15) are solved. For the fuel-lean case ($\alpha = 1$), fuel vapor is completely consumed at the flame front and only Eqs. (12), (14) and (15) are solved. In the following, we first present the analytical solutions for T, Y_O, and Y_d in the different zones (see Fig. 2). Then we derive the correlations which can determine the front of onset of liquid fuel vaporization and the spherical spray flame propagation speed as a function of flame radius. The solutions are presented directly in the following and the detailed derivation can be found in the Supplemental Document.

In the pre-vaporization zone ($\eta_v \leqslant \eta < \infty$), we have:

$$Y_d(\eta)=\delta \tag{25}$$

$$T(\eta)=T_v\cdot I_1(\eta,U)/I_1(\eta_v,U) \tag{26}$$

$$Y_O(\eta)=1-I_1(\eta,ULe_O)/I_1(0,ULe_O) \tag{27}$$

$$Y_F(\eta)=1-\delta+[\delta-1+Le_FDa\delta\cdot I_2(0,ULe_F)]\cdot I_1(\eta,ULe_F)/I_1(0,ULe_F) \tag{28}$$

where $I_1(x,\kappa)=e^{-\kappa R_f}\int_x^{\infty}(\xi+R_f)^{-2}e^{-\kappa\xi}d\xi$, and $I_2(x,\kappa)=e^{-\kappa R_f}\int_x^{\eta_v}(\xi+R_f)^{-2}e^{-\kappa\xi}\cdot E(\kappa,\xi,\eta_v)d\xi$. The evaporation-related integral, $E(x,\kappa_1,\kappa_2)$, is defined as

$$E(x,\kappa_1,\kappa_2)=\int_{\kappa_1}^{\kappa_2}\{(\xi+R_f)^2\exp[x(\xi+R_f)+Da(\xi-\eta_v)/U]\}d\xi \tag{29}$$

In the pre-flame zone ($0 \leqslant \eta < \eta_v$), the solutions are:

$$Y_d(\eta)=\delta\exp[Da(\eta-\eta_v)/U] \tag{30}$$

$$T(\eta)=T_v\cdot I_1(\eta,U)/I_1(\eta_v,U)+q_vDa\delta\cdot I_2(\eta,U) \tag{31}$$

$$Y_O(\eta) = 1 - I_1(\eta, ULe_O)/I_1(0, ULe_O) \tag{32}$$

$$Y_F(\eta) = 1 - \delta + [\delta - 1 + Le_F Da\delta \cdot I_2(0, ULe_F)] \cdot I_1(\eta, ULe_F)/I_1(0, ULe_F) - Le_F Da\delta I_2(\eta, ULe_F) \tag{33}$$

In the post-flame zone ($-R_f \leqslant \eta < 0$), we have:

$$Y_d(\eta) = \delta \exp[Da(\eta - \eta_v)/U] \tag{34}$$

$$T(\eta) = T_f + Q\int_\eta^0 (\xi + R_f)^{-2} e^{-U(\xi+R_f)} d\xi - (q_v - \alpha) \cdot Da\delta \int_\eta^0 \{(\xi + R_f)^{-2} e^{-U(\xi+R_f)} \cdot E(U, -R_f, \xi)\} d\xi \tag{35}$$

$$Y_F^\alpha(\eta) \times Y_O^{1-\alpha}(\eta) = 0 \tag{36}$$

Continuity of the temperature at flame front leads to the following implicit expression to determine the front of onset of vaporization (η_v):

$$T_f = T_v \cdot I_1(0, U)/I_1(\eta_v, U) + q_v Da\delta \cdot I_2(0, U) \tag{37}$$

By using the jump relations in Eq. (24), one obtains the following algebraic system for the fuel-rich case ($\alpha = 0$):

$$\begin{aligned} &\underbrace{T_f R_f^{-2} e^{-UR_f}/I_1(0,U)}_{\text{heat absorbed by gaseous fuel}} - \underbrace{QR_f^{-2}e^{-UR_f}}_{\text{heat provided by ignition energy}} \\ &\quad + \underbrace{q_v Da\delta R_f^{-2} e^{-UR_f}[E(U,-R_f,\eta_v) - I_2(0,U)/I_1(0,U)]}_{\text{heat absorbed for droplet evaporation}} \\ &= \underbrace{Le_O^{-1} R_f^{-2} e^{-UR_f}/I_1(0, ULe_O)}_{\text{heat supplied by oxygen}} \\ &= \underbrace{[\sigma + (1-\sigma)T_f]^2 \exp\{Z(T_f - 1)/[2\sigma + 2(1-\sigma)T_f]\}}_{\text{heat producted by reaction}} \end{aligned} \tag{38}$$

and the following one for the fuel-lean case ($\alpha = 1$):

$$\begin{aligned} &\underbrace{T_f R_f^{-2} e^{-UR_f}/I_1(0,U)}_{\text{heat absorbed by gaseous fuel}} - \underbrace{QR_f^{-2}e^{-UR_f}}_{\text{heat provided by ignition energy}} \\ &\quad - \underbrace{Da\delta R_f^{-2} e^{-UR_f} E(U,-R_f,0)}_{\text{heat supplied by droplet burning}} \\ &\quad + \underbrace{q_v Da\delta R_f^{-2} e^{-UR_f}[E(U,-R_f,\eta_v) - I_2(0,U)/I_1(0,U)]}_{\text{heat absorbed for droplet evaporation}} \\ &= \underbrace{(1-\delta) Le_F^{-1} R_f^{-2} e^{-ULe_F R_f}/I_1(0, ULe_F)}_{\text{heat supplied by initial fuel vapor}} \\ &\quad + \underbrace{Da\delta R_f^{-2} e^{-ULe_F R_f}[E(ULe_F, 0, \eta_v) - I_2(0, ULe_F)/I_1(0, ULe_F)]}_{\text{heat supplied by fuel vapor from droplet evaporation}} \\ &= \underbrace{[\sigma + (1-\sigma)T_f]^2 \exp\{Z(T_f - 1)/[2\sigma + 2(1-\sigma)T_f]\}}_{\text{heat producted by reaction}} \end{aligned} \tag{39}$$

In order to better understand Eqs. (38) and (39), the physical meaning of each term is identified. By numerically solving Eqs. (38) or (39), we can obtain the flame propagation speed, U, and flame temperature, T_f, as a function of flame radius, R_f, at any specified values for Q, δ, Da, and Le_O or Le_F. Therefore, the influence of initial droplet load, δ, and vaporization Damköhler number, Da, on spherical spray flame ignition and propagation can be assessed at different values of Lewis number and ignition power.

The present analysis can recover results for outwardly propagating spherical flames and planar flames in different limits. The detailed derivation is presented in the Supplementary Document. In the limit of zero droplet load (i.e. $\delta = 0$), Eq. (39) reduces to previous results on purely gaseous spherical flame [37,49]. In the limit of zero ignition power (i.e. $Q = 0$), the present result, Eq. (38), reduces to Greenberg's theory on freely propagating spherical spray flame in the adiabatic and quasi-steady limit [12–16]. It is noted that since the present analysis is based on the thermo-diffusive model rather than slowly varying flame model employed in Greenberg's analysis, there are some difference between the present results and Greenberg's [12–16]. In the limit of infinite large flame radius (i.e. $R_f \to \infty$), the present result reduces to that for planar spray flame. Therefore, the present analysis is consistent with previous studies in different limits ($\delta = 0$, $Q = 0$, or $R_f \to \infty$).

3. Results and discussion

This study is focused on examining the effects of finite-rate droplet evaporation on spherical spray flame initiation and propagation. In the following, the results of flame propagation speed, Markstein length, and critical ignition condition at different values of initial droplet load, vaporization Damköhler number, and Lewis number are presented for both fuel-rich and fuel-lean cases. The Zel'dovich number, $Z = 10$, and thermal expansion ratio, $\sigma = 0.15$, normalized boiling point of liquid fuel, $T_v = 0.15$, and normalized latent heat of vaporization, $q_v = 0.1$, are fixed (these values are chosen for typical fuels according to Lefebvre [50]).

3.1. Spherical spray flame propagation

The flame kernel generated by ignition power deposition is highly stretched; and its propagation speed depends strongly on the Markstein length [37,48,49]. Therefore, understanding the stretched flame propagation speed and Markstein length is crucial for examining the critical ignition condition in spray combustion. Here we first consider the freely propagating spherical spray flame without ignition power deposition at the center (i.e. $Q = 0$ in Eqs. (38) and (39)).

3.1.1. Stretched flame propagation speed

Figure 3 shows the flame propagation speed, U, and flame temperature, T_f, as a function of flame radius, R_f, for different values of droplet load, δ, and vaporization Damköhler number, Da. The results are plotted for R_f in the range of 0–1000. Nevertheless, the theoretical analysis works not only for $0 < R_f < 1000$, but also for $R_f > 1000$. It is observed the results are nearly independent of flame radius when R_f is close to 1000, indicating that the results for planar spray flame are approached. It is noted that practically the 1-D spherical spray flame with very large flame radius cannot be observed due to flame instability. Figure 3 shows that flame speed of 1-D spherical spray flame is always lower than that in the corresponding gaseous fuel-air mixture (i.e., $U < 1$). This is reasonable since we consider the off-stoichiometric mixtures, which remain to be fuel-lean or fuel-rich even after all the fuel droplets are vaporized. In previous studies [11,30], the flame speed in a spray was found to be higher than that in the corresponding gaseous fuel-air mixture. This was attributed to the wrinkling of the flame by the droplets which increased the flame surface area and promoted flame propagation [11,30]. Since the present theoretical analysis only considers 1-D spherical spray flame, the effect of flame instability on flame speed is not included and we always have $U < 1$ for $\delta > 0$.

For the fuel-rich case, Fig. 3(a) indicates that both U and T_f decrease with the initial droplet load, δ, when Da is fixed. This is due to the fact that droplet evaporation absorbs heat and thus reduces the flame strength/temperature. The same trend was observed in the theoretical studies considering infinite and finite vaporization rate by Greenberg [12,14]. At the same value of δ, Fig. 3(a) shows that both U and T_f decrease with the increase of

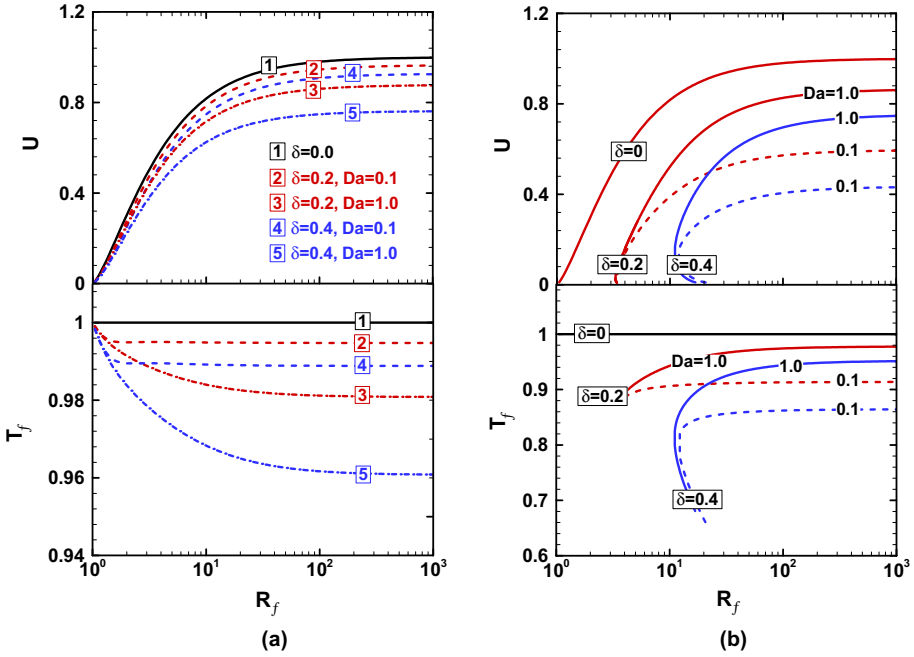

Fig. 3. Change of flame propagation speed U and flame temperature T_f with flame radius R_f: (a) fuel-rich case with $Le_O = 1.0$; (b) fuel-lean case with $Le_F = 1.0$.

Da. This is reasonable since faster vaporization at larger *Da* induces more latent heat of vaporization absorbed in the pre-flame zone. Moreover, Fig. 3(a) indicates that the flame ball solution (i.e., $U = 0$ at $R_f = 1$) is not affected by the initial droplet load for fuel-rich case.

For the fuel-lean case, Fig. 3(b) shows that both U and T_f also decrease with the initial droplet load, δ, when *Da* is fixed. It is noted that the total fuel mass fraction (i.e., both fuel droplet and fuel vapor) is fixed and thereby the local effective equivalence ratio (defined based on the fuel vapor only) reduces with the increase of droplet load for fuel-lean case. Consequently, the spherical spray flame is weakened by droplet load through (1) heat absorption for droplet evaporation and (2) reduction in local effective equivalence ratio. At relative low vaporization rate with $Da = 0.1$, both U and T_f decreases significantly with the increase of droplet load and are much lower than the counterparts for fuel-rich case shown in Fig. 3(a). Unlike the fuel-rich case, Fig. 3(b) shows both U and T_f increase with *Da* for fuel-lean case. This is due to the fact that faster vaporization at lager *Da* increases the local effective equivalence ratio (which dominates over the latent heat of vaporization absorbed in the pre-flame zone) and thus makes the flame become stronger.

Moreover, it is observed in Fig. 3(b) that with the increase of the initial droplet load, a *C*-shaped solution curve appears and the critical flame radius R_C (below which no solution exists) [49,51] increases. In order to explain this observation in Fig. 3(b), the distributions of gaseous fuel and liquid fuel mass fractions and temperature at $Le_F = 1$ are plotted in Fig. 4. For purely gaseous flame ($\delta = 0$), Fig. 4(a) shows that the characteristic thicknesses for heat diffusion, Δ_T, is equal to that for mass diffusion, Δ_M. This is reasonable since $Le_F = \Delta_T/\Delta_M$ [36]. However, for spray combustion ($\delta > 0$), Fig. 4(b) and (c) show that Δ_M, is smaller than Δ_T, indicating that the effective Lewis number is larger than unity. Therefore, for fuel-lean case, the presence of fuel droplets significantly increases the effective Lewis number, which results in the *C*-shaped U-R_f solution curve shown in Fig. 3(b). This observation is consistent with previous studies on purely gaseous spherical flame [37,49] which show that *C*-shaped U-R_f curve is observed for mixture with high Lewis number.

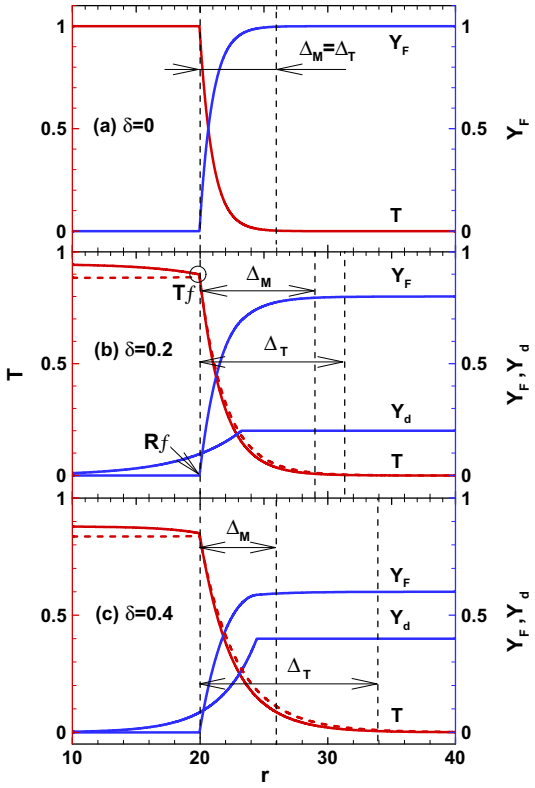

Fig. 4. The distributions of Y_F, Y_d and T for fuel-lean case with $Le_F = 1.0$, $R_f = 20$ and $Da = 0.1$. For the temperature, the solid lines stand for results considering droplet burning in the post-flame zone and the dashed lines for results neglecting droplet burning in the post-flame zone.

For the results discussed above, the Lewis number is fixed to be unity. The dependence of droplets effect on the Lewis number of oxygen (for fuel-rich case) or that of fuel (for fuel-lean case) is demonstrated in Fig. 5. The results in Fig. 5(a) and Fig. 3(a) indicate that the influence of vaporization Damköhler number on spherical

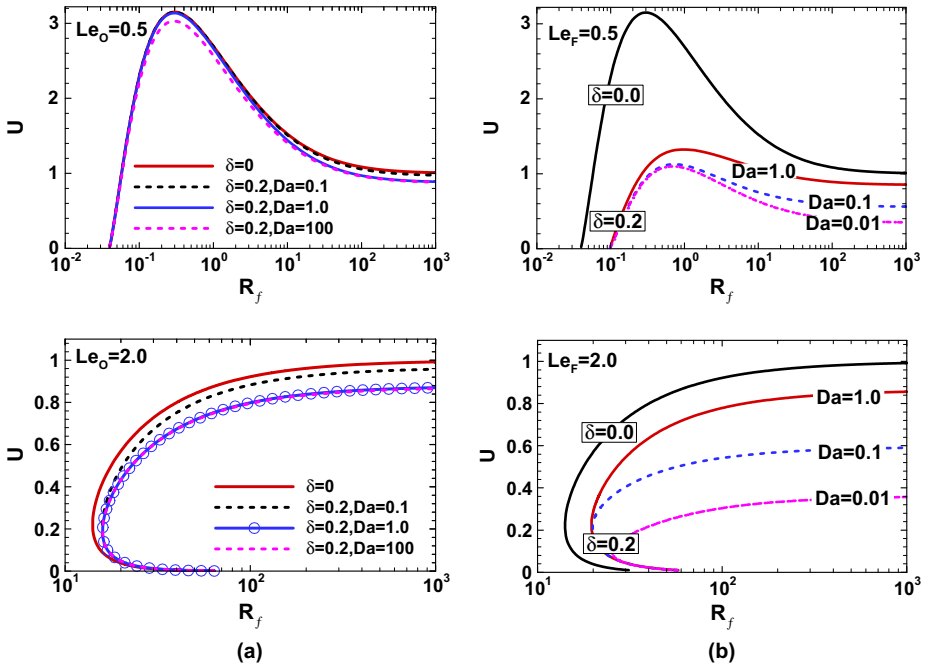

Fig. 5. Change of flame propagation speed U and flame temperature T_f with flame radius R_f: (a) fuel-rich case with $Le_O = 0.5$ and 2.0; (b) fuel-lean case with $Le_F = 0.5$ and 2.0.

flame propagation speed depends strongly on the Lewis number and flame radius. At $Da = 0.1$, the droplet evaporation (δ changes from 0 to 0.2) has little influence on flame propagation speed for $Le_O = 0.5$ while it obviously reduces the flame propagation speed for $Le_O = 2.0$. Moreover, Fig. 5(a) shows that when Da is increased from 1.0 to 100, the flame speed for $0.1 < R_f < 2$ and $Le_O = 0.5$ is reduced while that for $R_f > 2$ and $Le_O = 0.5$ and $Le_O = 2.0$ remains unchanged.

In order to explain the observations for the fuel-rich case in Figs. 3(a) and 5(a), we examine the amount of evaporation in the pre-flame zone defined as $f_1 = Y_d(R_v) - Y_d(R_f)$ and that in post-flame zone defined as $f_2 = Y_d(R_f) - Y_d(0)$. The total evaporation amount is $f = f_1 + f_2$. The results for $Le_O = 0.5$ are shown in Fig. 6. Evaporation in the pre-flame zone, f_1, reduces the temperature of the pre-mixture due to the latent heat for vaporization. Therefore, it directly reduces the flame temperature and flame speed. On the other hand, evaporation in the post-flame zone (i.e. f_2) results in heat flux from the flame front to the post flame zone and thereby indirectly weakens the flame. As a result, the flame propagation is mainly affected by evaporation in the pre-flame zone. Figure 6(a) shows that most of the droplets vaporize in the post-flame zone for $Da = 0.1$. Therefore, as shown in Fig. 5(a) for $Le_O = 0.5$, the flame propagation speed is nearly unaffected by droplet evaporation at $Da = 0.1$. With the increase of Da, Fig. 6(b) and (c) indicates that more droplets are evaporated into fuel vapor in the pre-flame zone (the droplets are completely evaporated in the preheat zone when $Da = 100$). When the value of Da is increased (from 1.0 to 10 or 100) and the flame radius is small ($0.1 < R_f < 2$), Fig. 6(b) and (c) shows that the amount of evaporation in the pre-flame zone increases greatly. Therefore, the flame propagation speed is reduced as shown in Fig. 5(a). Similar analysis also works for $Le_O = 2.0$.

Unlike the fuel-rich case, Fig. 5(b) shows that for the fuel-lean case, the difference between purely gaseous flame ($\delta = 0$) and spray flame ($\delta = 0.2$) becomes more significant at lower Lewis number (e.g. $Le_F = 0.5$) and smaller flame radius. Moreover, the influence of vaporization Damköhler number on flame propagation speed is shown to increase with the fuel Lewis number and it is much

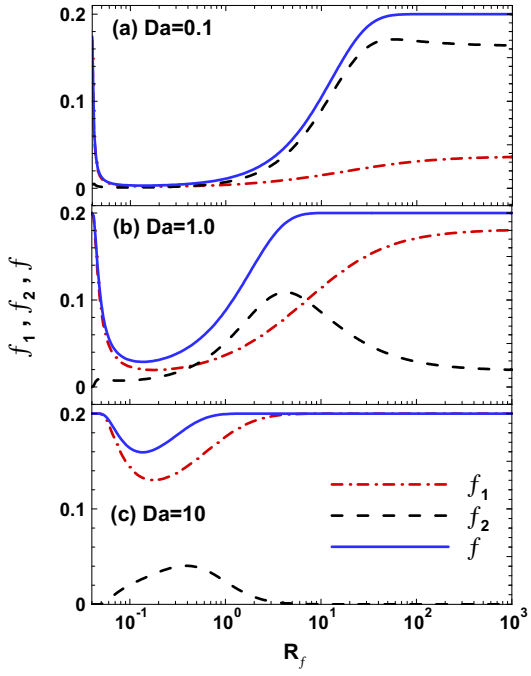

Fig. 6. Change of the amount of evaporation with flame radius for fuel-rich case with $Le_O = 0.5$ and $\delta = 0.2$.

stronger than that in the fuel-rich case. This is because at higher Lewis number, the positively stretched flame becomes weaker and thereby the change in local effective equivalence ratio by fuel vaporization rate (depends on Da) has stronger influence for fuel-lean case. According to the results in Figs. 3 and 5, the influence of initial droplet load and vaporization Damköhler number on spherical spray flame propagation depends on the Lewis number of oxygen (for fuel-rich case) or fuel (for fuel-lean case).

As mentioned in Section 1, heterogeneous combustion mode occurs when the surviving droplets (due to finite-rate

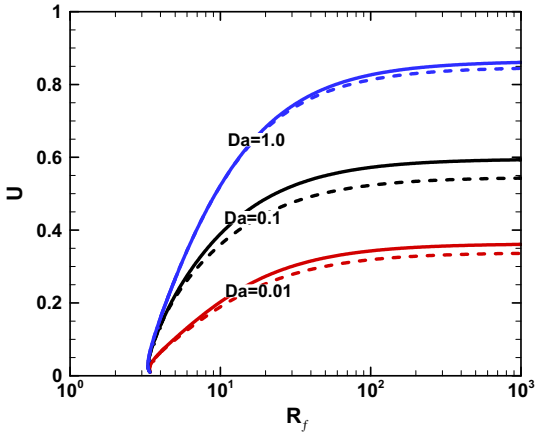

Fig. 7. Spherical flame propagation speed as a function of flame radius for fuel-lean case with $Le_F = 1.0$ and $\delta = 0.2$. The solid lines stand for results considering droplet burning in the post-flame zone and the dashed lines for results neglecting droplet burning in the post-flame zone.

vaporization) pass through the reaction layer in fuel-lean case (for which there is oxygen available in the post-flame zone). Droplet burning in the post-flame zone is essentially controlled by droplet evaporation rate at which fuel vapor is produced to sustain the diffusion flame surrounding each droplet. The temperature distribution in Fig. 4 shows that droplet burning in the post-flame zone results in gradual temperature rise. The effects of droplet burning on flame propagation speed are demonstrated in Fig. 7. The flame propagation speed is shown to be only slightly under-predicted if the droplet burning in the post-flame zone is neglected. Moreover, this under-prediction is show to increase with flame radius. This is because the length of post-flame zone is equal to the flame radius and more droplet burning occurs at larger flame radius.

3.1.2. Markstein length

Up to this point, the effects of droplet evaporation on the propagation speed of the spherical spray flame have been examined. In the following we investigate another important parameter, Markstein length, L, which characterizes the variation in the local flame speed due to the influence of external stretching [36].

Figure 8 shows the flame propagation speed as a function of stretch rate (which is $K = 2U/R$ for outwardly propagating spherical flame). It is observed that the U–K curve is much more greatly affected by droplet evaporation for fuel-lean case than for fuel-rich case. There exists a maximum stretch rate beyond which no propagating spherical flame exists. This maximum stretch rate is called as the extinction stretch rate for spherical flame propagation [40,52]. As shown in Fig. 8, droplet evaporation reduces the extinction stretch rate, especially for the fuel-lean case. This is reasonable since the effective Lewis number for the fuel-lean case increases greatly with droplet load and the extinction stretch rate decreases with the Lewis number [40]. Moreover, Fig. 8 indicates linear change between U and K at low stretch rate. Therefore, similar to the purely gaseous flame, the Markstein length of the spray flame, L, can also be obtained from the linear extrapolation according to $U = U^0 - L \cdot K$, where U^0 is the flame speed at zero stretch rate (i.e. for planar flame at $R_f \to \infty$).

Figure 9 demonstrates that the Markstein length is affected by the initial droplet load and vaporization Damköhler number. For fuel-rich case, Fig. 9(a) shows that the negative Markstein length at $Le_O < 1.0$ becomes smaller at larger value of droplet load or vaporization Damköhler number; while the positive Markstein length at $Le_O > 1.0$ increases with δ or Da. Therefore, the absolute value of Markstein length is enlarged by droplet evaporation, indicating that the influence of external stretching becomes stronger when droplet evaporation is considered (i.e., spray flame is more sensitive to flame stretch than gaseous flame). This is due to the fact that latent heat of vaporization absorbed in the pre-flame zone makes the flame weaker and weaker flame is more sensitive to stretch rate [36]. The influence of droplet evaporation is similar to that of radiative loss which also weakens the flame and increases the absolute value of Markstein length [39]. Furthermore, Fig. 9 shows that the influence of droplet evaporation on Markstein length depends on the Lewis number: it is negligible for mixtures with Lewis number close to unity and only important for mixtures with Lewis number appreciably different from unity. Similar behavior was also observed for the influence of radiative loss on Markstein length [39].

Unlike the fuel-rich case, Fig. 9(b) shows that the Markstein length in the fuel-lean case with $Da = 1.0$ increase greatly with the initial droplet load. This is because larger droplet load results in higher effective Lewis number. At fixed initial droplet load of $\delta = 0.2$, the Markstein length is affected by vaporization Damköhler number in the same trend for fuel-lean and fuel-rich cases. Compared to the fuel-rich case, the influence of droplet evaporation on Markstein length becomes much stronger for fuel-lean case.

The above discussion shows that droplet evaporation has different influence on Markstein length for fuel-rich and fuel-lean cases and the influence depends on Lewis number. Since ignition strongly depends on the Markstein length [37,49], it is expected that the critical ignition condition is also affected by droplet evaporation. This is demonstrated in the following subsection.

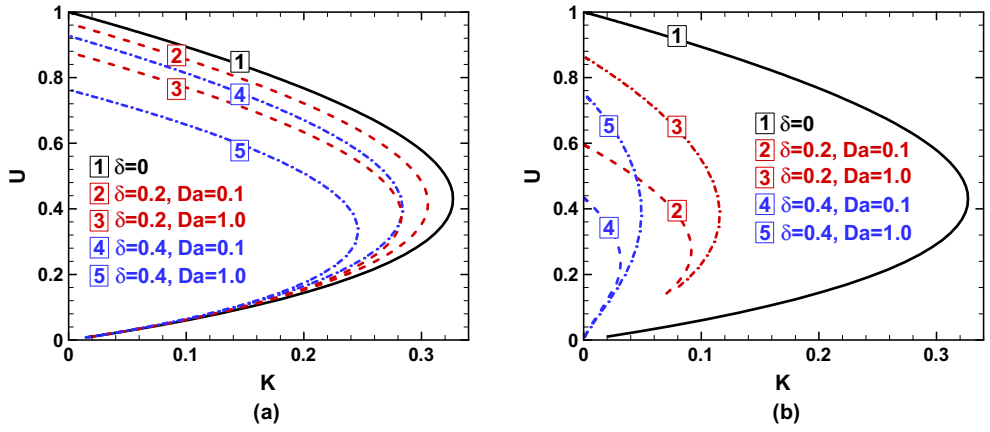

Fig. 8. Flame propagating speed U as a function of stretch rate K: (a) fuel-rich case with $Le_O = 1.0$; (b) fuel-lean case with $Le_F = 1.0$.

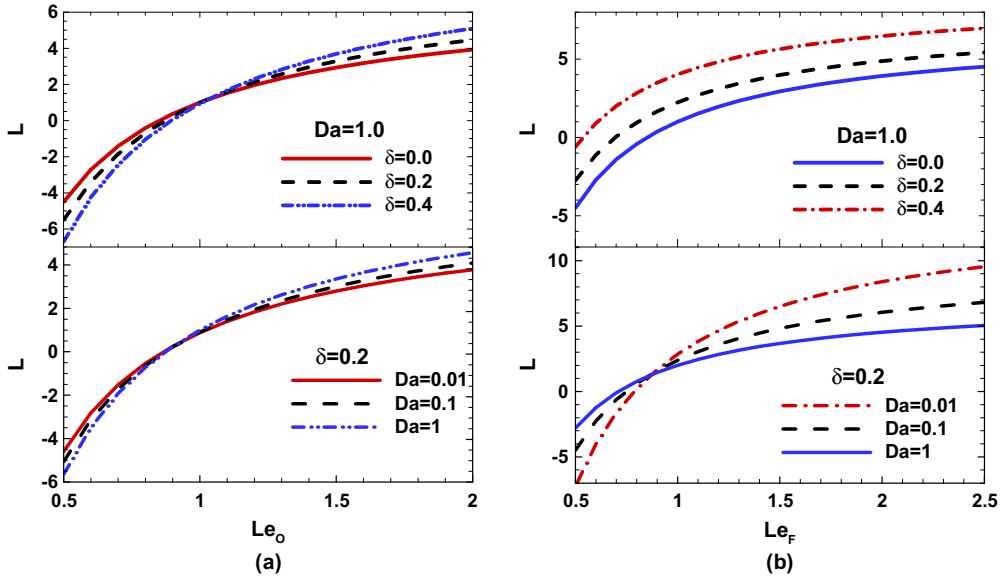

Fig. 9. Markstein length as a function of Lewis number for fuel-rich (a) and fuel-lean (b) cases.

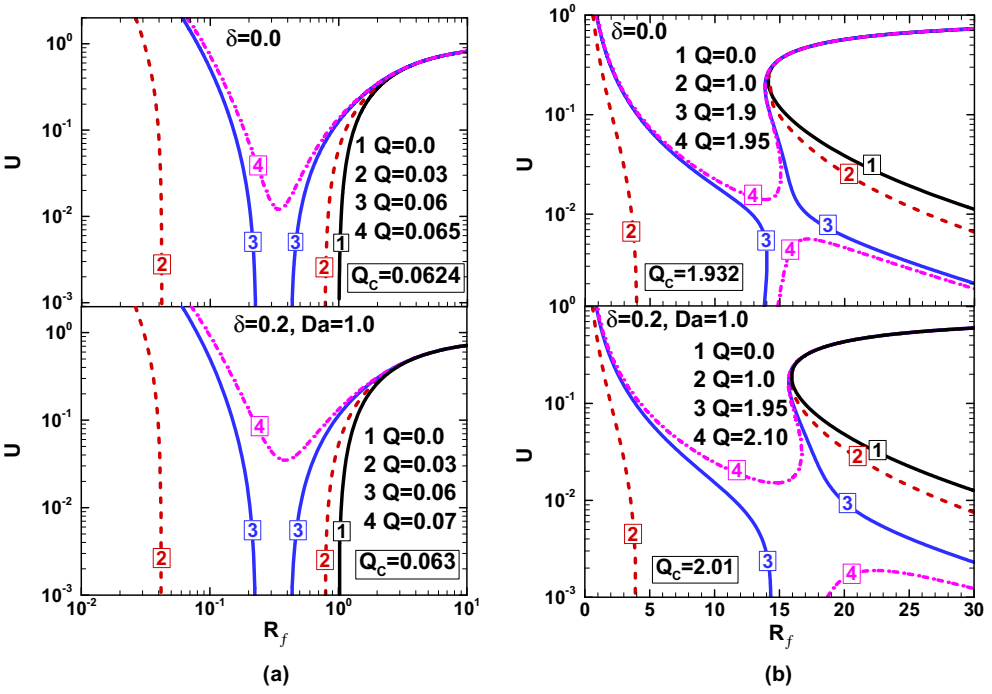

Fig. 10. Flame propagating speed U as a function of flame radius R_f at different ignition powers at (a) $Le_O = 1.0$ and (b) $Le_O = 2.0$ for fuel-rich case.

3.2. Spherical spray flame initiation

With the help of Eqs. (38) and (39), we examine the influence of droplet evaporation on the ignition kernel development and critical ignition condition.

The spherical flame propagation speed as a function of flame radius at different ignition powers is shown in Fig. 10 for the fuel-rich case. The results for purely gaseous flame ($\delta = 0$) are the same as those in [37,49] and they are presented here for comparison with spherical spray flame ($\delta = 0.2$). Figure 10(a) compares the results without and with the droplet evaporation ($\delta = 0$ and $\delta = 0.2$) at $Le_O = 1.0$. When there is no ignition power deposition at the center (i.e. $Q = 0$), the results are the same as those in Fig. 3(a) and the outwardly propagating spherical flame only exists when the flame radius is larger than the flame ball radius. When a small external power is deposited at the center (lines 2 in Fig. 10(a)), there exists two branches of solutions: the original traveling flame branch on the right and a new ignition kernel branch on the left. Once the external power is larger than the minimum ignition power, Q_C, the left ignition kernel branch merges with the right traveling flame branch, resulting in a new upper branch along which successful ignition can be achieved. For $\delta = 0$, the minimum ignition power is $Q_C = 0.0624$; and for $\delta = 0.2$, it becomes $Q_C = 0.063$. Therefore, for $Le_O = 1.0$, the critical ignition power only

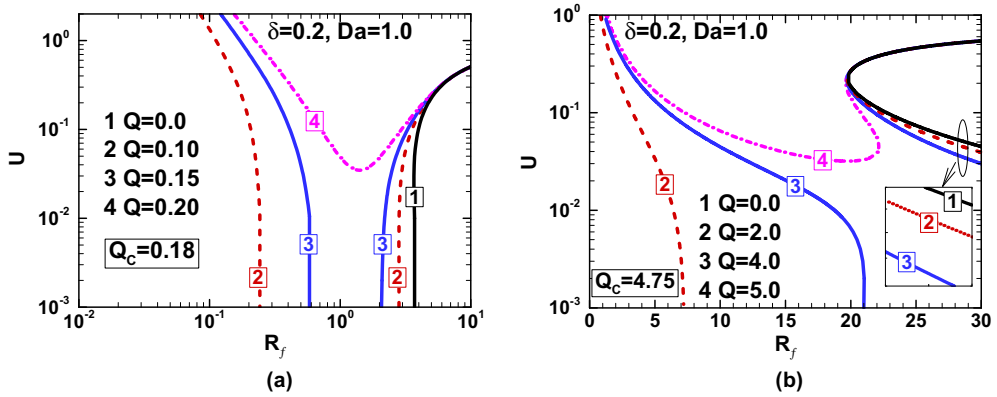

Fig. 11. Flame propagating speed U as a function of flame radius R_f at different ignition powers at (a) $Le_F = 1.0$ and (b) $Le_F = 2.0$ for fuel-lean case.

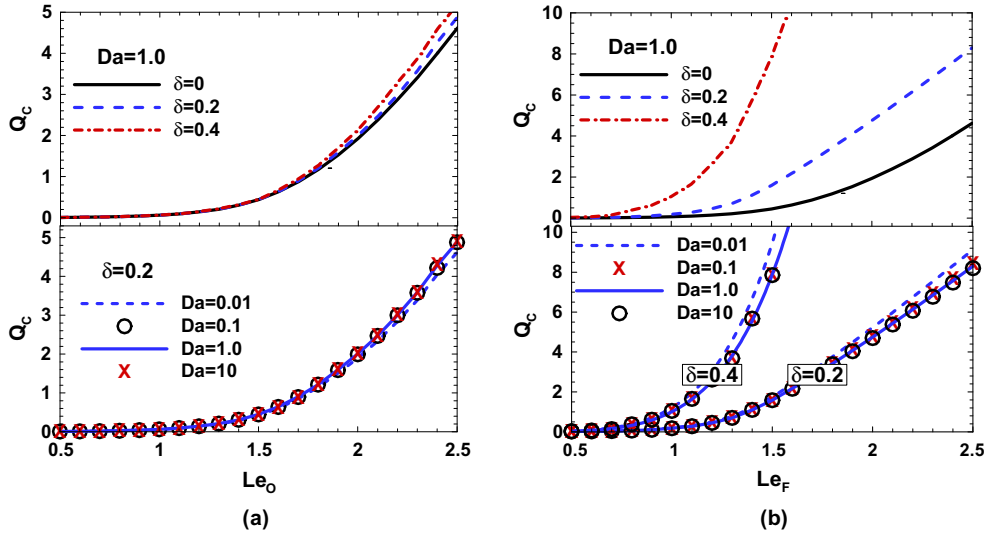

Fig. 12. Minimum ignition power Q_c as a function of Lewis number for fuel-rich (a) and fuel-lean (b) cases.

slightly increases (about 1%) when the droplet load is changed from $\delta = 0$ to $\delta = 0.2$. This is due to the facts that for $Le_O = 1.0$, both the critical flame radius (flame ball radius) (see Fig. 3a) and the Markstein length (see Fig. 9a) are almost unaffected by droplet evaporation for $Le_O = 1.0$.

For $Le_O = 2.0$, Fig. 10(b) shows that a C-shaped U-R branch (line 1) is observed for $Q = 0$. When the ignition power is introduced (lines 2 and 3 in Fig. 10(b)), an ignition-kernel branch appears on the left with a turning point corresponding to the maximum possible flame radius. Again, successful ignition is achieved once the left and right U-R branches merge with each other, which occurs for $Q > Q_C$. Comparison between the purely gaseous flame and the spray flame indicates that droplet evaporation does not qualitatively affect the ignition process. However, unlike the case of $Le_O = 1.0$, both the critical flame radius (see Fig. 5a) and the Markstein length (see Fig. 9a) are enlarged by droplet evaporation for $Le_O = 2.0$. Consequently, for $Le_O = 2.0$ the minimum ignition power increases by 4.0% when the droplet load is changed from $\delta = 0$ to $\delta = 0.2$.

Similar results are shown in Fig. 11 for the fuel-lean case (the results for purely gaseous flame with $\delta = 0$ is the same as those for the fuel-rich case, as shown in Fig. 10). Compared to the fuel-rich case, droplet evaporation has much stronger influence on the ignition for fuel-lean case: the minimum ignition power increases by 188% (=0.18/0.0624-1) for $Le_F = 1.0$ and by 146% (=4.75/1.932-1) for $Le_F = 2.0$ when the droplet load is changed from $\delta = 0$ to $\delta = 0.2$. This is due to the facts that the flame propagation speed is greatly reduced by droplet load and that both the critical flame radius and the Markstein length increase when droplets vaporization are taken into account (see Figs. 3b, 5b and 9b). All these changes make the ignition becomes more difficult [49].

Figure 12 illustrates the dependence of the minimum ignition power on Lewis number at different values of initial droplet load and vaporization Damköhler number. For both gaseous ($\delta = 0$) and spray ($\delta > 0$) flames, the minimum ignition power always monotonically increase with Lewis number. This is due to the fact that for the highly positively-stretched spherical ignition kernel, the increase in Lewis number reduces the flame propagation speed and thus hinders the ignition process [37,48,49]. For the fuel-rich case, Fig. 12(a) shows that the minimum ignition power is slightly affected by droplet load only when the Lewis number is above 1.5. The maximum relative change in Q_c occurs at largest Lewis number and it is 12.5% for $\delta = 0.4$ and $Le_O = 2.5$. Moreover, Fig. 12(a) also indicates that Q_c increases with vaporization Damköhler number and the increment is negligible for the larger Da. This is because the ignition kernel has high flame temperature and thereby very broad vaporization zone, which makes the droplet completely evaporated in the pre-flame zone even for small Da (i.e., low vaporization rate).

Please cite this article in press as: W. Han, Z. Chen, Combust. Flame (2015), http://dx.doi.org/10.1016/j.combustflame.2015.01.011

For the fuel-lean case, Fig. 12(b) shows that the minimum ignition power increases significantly with droplet load, especially at large Lewis number. Therefore, for hydrocarbon fuels with large Lewis number, the lean spray flame is much more difficult to be successfully ignited compare to the equivalent purely gaseous flame. Since the high-altitude relight occurs at fuel-lean case and Lewis number of jet fuel is large, much more ignition power should be deposited to successfully initialize the spray flame. Moreover, similar to the fuel-rich case, Fig. 12(b) indicates that for fuel-lean case the vaporization Damköhler number also has much smaller influence on the minimum ignition power than the initial droplet load.

4. Conclusions

A simplified theoretical model for spherical spray flame initiation and propagation is analyzed in this study. Fuel-rich and fuel-lean mixtures containing fuel droplet with finite-rate evaporation, fuel vapor, and air are considered and quasi-steady spherical flame propagation is assumed. Large-activation-energy asymptotic analysis is conducted and analytical correlations describing spherical spray flame initiation and propagation at different vaporization parameters, Lewis numbers, and ignition powers are derived. Based on these correlations, the effects of droplet evaporation on spherical spray flame propagation speed, Markstein length, and minimum ignition power are assessed. The main conclusions are:

1. For the fuel-rich case, the spherical spray flame is affected by droplet evaporation only through latent heat of vaporization absorbed in the pre-flame and post-flame zones. Therefore, the spherical spray flame propagation speed decreases with both initial droplet load and vaporization Damköhler number. Unlike the flame propagation speed, the absolute value of Markstein length increases with initial droplet load and vaporization Damköhler number, indicating that spray flame is more sensitive to external stretching than purely gaseous flame. For the ignition process, droplet evaporation does not qualitatively affect the ignition kernel development. The minimum ignition power is slightly affected (below 12.5% for $\delta \leqslant 0.4$) by droplet load and the influence depends on the Lewis number. Furthermore, the Damköhler number has little influence on the minimum ignition power since the high flame temperature of ignition kernel ensures complete evaporation in the preheat zone.
2. For the fuel-lean case, the spherical spray flame is affected by droplet evaporation through (1) latent heat of vaporization absorbed in the pre-flame and post-flame zones and (2) change in local effective equivalence ratio. Therefore, the flame propagation speed decreases greatly with initial droplet load and increases with vaporization Damköhler number. The flame propagation speed is only slightly under-predicted if the droplet burning in the post-flame zone is neglected. The presence of fuel droplets significantly increases the effective Lewis number, which causes great increase in the Markstein length and minimum ignition power. The minimum ignition power can be increased by more than 100% for $\delta = 0.2$ and $Le_F > 1.5$. It is very difficult to successfully ignite lean spray flame for hydrocarbon fuels with large Lewis number.

It is noted that the present analysis is based on the assumptions of one-step irreversible reaction with large activation energy, thermal-diffusive approximation with constant density, and quasi-mono-disperse model for the spray. Moreover, the droplets are viewed from a far-field vantage point (i.e., in the dilute spray region and droplets very small) and are considered to be dilute (i.e., its volume fraction is relatively small). Therefore, the above conclusions only hold for fast chemistry with low heat release and dilute droplets with low droplet load. Besides, the detailed heat transfer between droplet and gas phase is not considered and the viscosity of the liquid and interactions among the droplets are neglected. Numerical simulations need to be conducted so that less severe assumptions can be made and quantitative information can be provided for the ignition and propagation of premixed spherical spray flame.

Acknowledgment

This work was supported by National Natural Science Foundation of China (Nos. 51322602 and 51136005).

Appendix A. Supplementary material

Supplementary data associated with this article can be found, in the online version, at http://dx.doi.org/10.1016/j.combustflame.2015.01.011.

References

[1] G. Continillo, W.A. Sirignano, Proc. Combust. Inst. 22 (1989) 1941–1949.
[2] G. Continillo, W.A. Sirignano, Modern Reserach Topics in Aerospace Propulsion, Springer-Verlage, 1991.
[3] H.H. Chiu, C.L. Lin, Proc. Combust. Inst. 26 (1996) 1653–1661.
[4] T.H. Lin, C.K. Law, S.H. Chung, Int. J. Heat Mass Transfer 31 (1988) 1023–1034.
[5] T.H. Lin, Y.Y. Sheu, Combust. Flame 84 (1991) 333–342.
[6] J.B. Greenberg, A. Kalma, Int. J. Turbo Jet Engines 14 (1997) 201–216.
[7] J.B. Greenberg, A. Kalma, Int. J. Turbo Jet Engines 18 (2001) 65–76.
[8] I. Silverman, J.B. Greenberg, Y. Tambour, Combust. Flame 93 (1993) 97–118.
[9] D. Bradley, M. Lawes, S. Liao, A. Saat, Combust. Flame 161 (2014) 1620–1632.
[10] J.B. Greenberg, I. Silverman, Y. Tambour, Combust. Flame 104 (1996) 358–368.
[11] J.B. Greenberg, I. Silverman, Y. Tambour, Combust. Flame 113 (1998) 271–273.
[12] J.B. Greenberg, Combust. Theor. Model. 7 (2003) 1–12.
[13] K. Klots, J.B. Greenberg, Int. J. Turbo Jet Engines 22 (2005) 13–20.
[14] J. Greenberg, Combust. Flame 148 (2007) 187–197.
[15] J.B. Greenberg, L.S. Kagan, G.I. Sivashinsky, Int. J. Spray Combust. 2 (2010) 285–300.
[16] J.B. Greenberg, E. Mastorakos, Int. J. Spray Combust. 4 (2012) 97–122.
[17] J.B. Greenberg, A. Kalma, Combust. Flame 123 (2000) 421–429.
[18] K.V.L. Rao, A.H. Lefebvre, Combust. Flame 27 (1976) 1–20.
[19] D.R. Ballal, A.H. Lefebvre, Proc. R. Soc. London, Ser. A 364 (1978) 277–294.
[20] D.R. Ballal, A.H. Lefebvre, Combust. Flame 35 (1979).
[21] B. Seth, S.K. Aggarwal, W.A. Sirignano, Combust. Flame 39 (1980) 149–168.
[22] S.K. Aggarwal, W.A. Sirignano, Comput. Fluids 12 (1984) 145–158.
[23] S.K. Aggarwal, W.A. Sirignano, Combust. Flame 62 (1985) 69–84.
[24] S.K. Aggarwal, Prog. Energy Combust. Sci. 24 (1998) 565–600.
[25] A. Neophytou, E. Mastorakos, Combust. Flame 156 (2009) 1627–1640.
[26] A. Neophytou. Spark ignition and flame propagation in sprays. Ph.D. thesis, University of Cambridge, 2010.
[27] J.B. Greenberg, Int. J. Spray Combust. 1 (2009) 417–434.
[28] J.B. Greenberg, A.C. McIntosh, J. Brindley, Proc. R. Soc. London, Ser. A 457 (2001) 1–31.
[29] C. Nicoli, P. Haldenwang, S. Suard, Combust. Flame 143 (2005) 299–312.
[30] S. Hayashi, S. Kumagai, T. Sakai, Combust. Sci. Technol. 15 (1977) 169–177.
[31] Y. Tambour, Combust. Flame 58 (1984) 103–114.
[32] Y. Tambour, Combust. Flame 60 (1985) 15–28.
[33] J.B. Greenberg, N. Sarig, Proc. Combust. Inst. (1996) 1705–1711.
[34] C. Nicoli, P. Haldenwang, S. Suard, Combust. Flame 149 (2007) 295–313.
[35] G. Joulin, P. Clavin, Combust. Flame 35 (1979) 139–153.
[36] C.K. Law, Combustion Physics, Cambridge University Press, 2006.
[37] Z. Chen, Y. Ju, Combust. Theor. Model. 11 (2007) 427–453.
[38] Z. Chen, Y. Ju, Int. J. Heat Mass Transfer 51 (2008) 6118–6125.
[39] Z. Chen, X. Gou, Y. Ju, Combust. Sci. Technol. 182 (2010) 124–142.
[40] Y. Wu, Z. Chen, Acta Mech. Sin. 28 (2012) 359–366.
[41] J.B. Greenberg, R. Cohen, J. Eng. Math. 31 (1997) 397–409.
[42] C.K. Law, Combust. Sci. Technol. 15 (1977) 65–74.
[43] C.K. Law, W.A. Sirignano, Combust. Flame 28 (1977) 175–186.
[44] M. Labowsky, Combust. Sci. Technol. 22 (1980) 217–226.
[45] K. Annamalai, W. Ryan, Prog. Energy Combust. Sci. 18 (1992) 221–295.
[46] J.B. Greenberg, I. Silverman, Y. Tambour, Combust. Flame 93 (1993) 90–96.
[47] H. Zhang, Z. Chen, Combust. Flame 158 (2011) 1520–1531.
[48] H. Zhang, P. Guo, Z. Chen, Proc. Combust. Inst. 34 (2013) 3267–3275.
[49] Z. Chen, M.P. Burke, Y. Ju, Proc. Combust. Inst. 33 (2011) 1219–1226.
[50] A.H. Lefebvre, Atomization and Sprays, Taylor and Francis, USA, 1989.
[51] L. He, Combust. Theor. Model. 4 (2000) 159–172.
[52] D. Bradley, M. Lawes, M.S. Mansour, Combust. Flame 156 (2009) 1462–1470.
[53] W. Han, Z. Chen, Int. J. Heat Mass Transfer 82 (2015) 309–315, http://dx.doi.org/10.1016/j.ijheatmasstransfer.2014.11.062.